DYNAMIC MODEL OF ISOLATED PARAMETRIC GENERATOR WITH APPLICATION IN WIND ENERGY SYSTEMS

Essam El-Din M. Rashad
Electrical Engineering Department, Faculty of Engineering,
Tanta University, Tanta, EGYPT

ABSTRACT

This paper presents the development of a dynamic model for the three-phase self-excited stand-alone parametric generator. The derivation is based on the transformation of the actual machine dynamic equations into the synchronously rotating reference frame. Effect of magnetic saturation has been considered due to its well-known stabilizing action in self-excited generators. The results have been checked using an experimental setup. The model is then extended to the case of using a wind turbine as a prime mover. The dynamic behavior of the generator has been examined to show the effect of the turbine characteristics in comparison with the case of constant speed prime movers. The investigated dynamic behavior includes the voltage build-up as well as sudden change in load in the case of constant wind speed. The proposed dynamic model has been also employed to study the generator response under wind gusting conditions.

Keywords: Dynamics, Simulation, Parametric generator, Self-excitation, Wind energy.

LIST OF SYMBOLS

v_{as} , v_{bs} , v_{cs}	instantaneous stator phase voltages., V.
i_{as} , i_{bs} , i_{cs}	instantaneous stator phase currents, A.
v_{ar} , v_{br} , v_{cr}	instantaneous rotor phase voltages, V.
i_{ar} , i_{br} , i_{cr}	instantaneous rotor phase currents, A.
v_d , v_q	instantaneous transformed voltages, V.
i_d , i_q	instantaneous transformed currents,A.
R_a	equivalent phase resistance of the machine windings, Ω.
L_a	equivalent phase self inductance of the machine windings, H.
L_m	max. mutual inductance between one stator phase and one rotor phase, H.
θ	instantaneous electrical angle between stator phase 'a' and rotor phase 'a'.
ω	electrical angular frequency of the induced voltage, rad/s.
ω_{re}, ω_{rm}	electrical and mechanical generator angular shaft speeds, rad/s.
C	exciting phase capacitance, F.
N_r , N_t	generator and turbine shaft speeds, rpm.
P	number of generator poles
p	differential operator d/dt.

1- INTRODUCTION

In the last decades, attention has been paid to the renewable sources of energy such as sun, wind, ocean,...,etc. This is due to the rapid consumption of the conventional fossil types of fuel and the need of the nuclear fuels to a very complicated technology which is not available for most of the developing countries. So it is of prime importance to study the behavior of different types of electrical generators when used in conjunction with systems of renewable sources of energy.

The parametric generator is a type of self-excited generator that arose when studying the behavior of the *RLC* series circuit when one of its storage elements (*L* or *C*) is periodically varying with time. Actually, this type of machine is a conventional wound-rotor induction machine. Operation as a

parametric machine necessitates the series connection of the stator and rotor windings with proper relative phase sequence. As a generator, the self-excitation is possible when connecting a suitable capacitor bank across the machine terminals. The three-phase parametric generator has been introduced and analyzed using Floquet theory as well as the transformation to d-q model [1,2]. It was found that the parametric generator is inherently of synchronous type. The frequency of the generated emf is determined only by the number of poles and the prime mover speed. It is independent of the loading conditions in the stable range of operation. A salient feature of the parametric machines (motors and generators) is that the electromechanical energy conversion takes place only if:

1. The rotor speed is double the synchronous speed. This means that, for a P-pole machine, the relation between the speed N_r and the mmf frequency f is given by:

$$N_r = 2^* (120^* f/P) \qquad (1)$$

2. The series connection of the stator and rotor windings is such that the phase sequence of rotor mmf is in reverse sense to that of the stator mmf (Figure (1)).

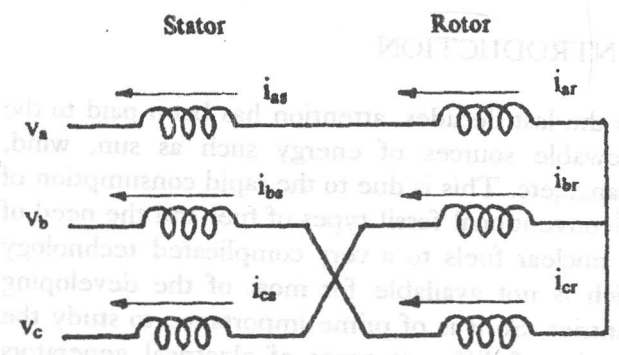

Figure 1. Series connection of the stator and rotor windings of the parametric machine.

The generator performance has been investigated with the aid of a suggested phasor diagram [3] and compared with the performance of the induction generator [4]. Voltage control of the parametric generator has been studied using both of capacitor and inductor control [5]. A fixed capacit thyristor-controlled reactor has been designed a applied to keep the terminal voltage constant wi the variation in load current [6].

The steady state performance of the machine the motor mode of operation has been investigat in a previous paper [7].

The previous published work in the field parametric generators was focused on t steady-state condition. So, the aim of this paper to:

- present a mathematical dynamic model for t generator in the case of stand-alone (isolate operation.
- check the validity of the model with the aid of experimental setup.
- apply the model to the case of using a wi turbine prime mover to study its effect on t dynamic behavior including voltage build-u sudden change in load and wind gusti conditions.

The results will be useful in selecting a designing the suitable control method to achie more satisfactory performance for the parameti generator.

2- GENERATOR DYNAMIC MODEL

The electrical system of the generator consists the following three parts:

1- The induction machine connected as a parameti machine.
2- The exciting capacitor bank.
3- The load.

All these parts are assumed to be of three-pha balanced configuration.

In deriving the full dynamic model of the electric system, the induction machine will be treated first as an individual part as will be shown .

2-1 *Machine Model*

Based on the proper electrical connection betwe stator and rotor windings, the voltage balan equation of the generator mode of operation can b written in the following operational matrix form:

$$V + Z(p)\, I = 0 \qquad (2)$$

where

$V = [\, v_a \; v_b \; v_c]^T$;

$$v_a = v_{as} + v_{ar},\; v_b = v_{bs} + v_{cr},\; v_c = v_{cs} + v_{br}$$

$I = [\, i_a \; i_b \; i_c]^T$;

$$i_a = i_{as} = i_{ar},\; i_b = i_{bs} = i_{cr},\; i_c = i_{cs} = i_{br}$$

$Z(p)$ is the transient impedance matrix =

$$\begin{bmatrix} R_a + p\{L_a + 2L_m\cos(\theta)\} & p\{-0.5L_a + 2L_m\cos(\theta-120^\circ)\} & p\{-0.5L_a + 2L_m\cos(\theta+120^\circ)\} \\ p\{-0.5L_a + 2L_m\cos(\theta-120^\circ)\} & R_a + p\{L_a + 2L_m\cos(\theta+120^\circ)\} & p\{-0.5L_a + 2L_m\cos(\theta)\} \\ p\{-0.5L_a + 2L_m\cos(\theta+120^\circ)\} & p\{-0.5L_a + 2L_m\cos(\theta)\} & R_a + p\{L_a + 2L_m\cos(\theta-120^\circ)\} \end{bmatrix}$$

In the absence of zero sequence quantities, the synchronously rotating reference frame transformation is given by:

$$K^T = \sqrt{2/3}\begin{bmatrix} \cos(\omega t) & \cos(\omega t - 2\pi/3) & \cos(\omega t + 2\pi/3) \\ \sin(\omega t) & \sin(\omega t - 2\pi/3) & \sin(\omega t + 2\pi/3) \end{bmatrix} \quad (3)$$

From eqn.(1) the electrical angular rotor speed ω_{re} ($=\dot{\theta}$) is double the mmf angular frequency Ω such that:

$$\omega_{re} = (P/2)\,\omega_{rm} = 2\,\omega \quad (4)$$

The transformed voltage balance equation is as follows:

$$\tilde{V} + \tilde{Z}(p)\tilde{I} = 0 \quad (5)$$

where:

$$\tilde{V} = [v_d \;\; v_q]^T \quad \tilde{I} = [i_d \;\; i_q]^T \text{ and}$$

$$\tilde{Z}(p) = \begin{bmatrix} R_a + L_d p & \omega L_q \\ -\omega L_d & R_a + L_q p \end{bmatrix}$$

$L_d = (3/2)\{L_a + 2L_m\}$ the direct axis inductance.

$L_q = (3/2)\{L_a - 2L_m\}$ the quadrature axis inductance.

The result is similar to that obtained for the reluctance machine. This shows that the parametric machine acts as a hypothetical salient-pole machine [1,2] which justifies its synchronous operation. Therefore both of reluctance and parametric machines can be treated using the same mathematical equations. This is restricted by the use of the proper definition of machine parameters as well as the relation between speed and frequency.

Rearranging eqn.(5) results in :

$$p\, i_d = \{-v_d - R_a\, i_d - \omega\, L_q\, i_q\}/L_d \quad (6)$$

$$p\, i_q = \{-v_q + \omega L_d\, i_d - R_a\, i_q\}/L_q \quad (7)$$

Equations (6) and (7) determine the machine currents for given terminal voltage. If the speed is assumed to be constant, the terminal voltage of the stand-alone generator is determined by the value of the excitation capacitance along with load conditions. However, if the prime mover does not guarantee constant-speed operation, the mechanical equation of motion should be also included.

2-2 *Full Electrical System Model*

To obtain the full model for the stand-alone generator, equations of the exciting capacitance and load are to be combined with the machine equations. To avoid transforming the capacitance and load branches, it is suggested to derive the full model from the actual quantities as follows.

Consider only one phase of the balanced system, say phase 'a' as shown in Figure (2). The actual phase voltage is related to the transformed voltage according to the relation:

$$v_a = \sqrt{2/3}\,\{v_d\cos(\omega t) + v_q\sin(\omega t)\} \quad (8)$$

Similarly:

$$i_a = \sqrt{2/3}\,\{i_d\cos(\omega t) + i_q\sin(\omega t)\} \quad (9)$$

Since $p\, v_a = i_{ca}/C$, then:

$$\sqrt{2/3}\,\{(-\omega v_d + p v_q)\sin(\omega t) + (\omega v_q + p\, v_d)\cos(\omega t)\} = (i_a - i_{La})/C \quad (10)$$

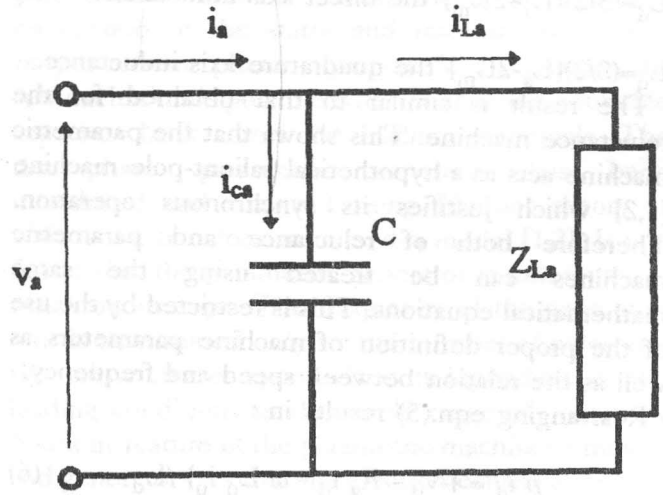

Figure 2. Terminal configuration of phase 'a'.

i) *Resistive load condition*

In this case, the load impedance per phase Z_L reduces to R_L such that:

$$i_{La} = v_a/R_L \qquad (11)$$

Using equations (6-10) and equating coefficients of sin(ωt) and cos(ωt) yield:

$$p\, v_d = -\omega\, v_q + i_d/C - v_d/(C\, R_L) \qquad (12)$$

$$p\, v_q = \omega\, v_d + i_q/C - v_q/(C\, R_L) \qquad (13)$$

Equations (6),(7),(12) and (13) represent the full mathematical model for the resistive load. No-load condition can be simply attained by letting R_L tend to infinity.

ii) *General Passive load condition*

To get a more general model, the load can be assumed to be represented by any combination of passive elements such that:

$$i_{La} = v_a/Z_L\,(p) \qquad (14)$$

where $Z_L\,(p)$ is the load impedance in the operational form.

Substituting from eqn.(8) in eqn.(14) yields:

$$i_{La} = \sqrt{2/3}\,\frac{1}{Z_L(p)}\,\{v_d \cos(\omega t) + v_q \sin(\omega t)\} \qquad (1$$

Under steady-state conditions, both v_d and v_q constants. To simplify the analysis, v_d and v_q assumed to be constants during each step integration. Under this assumption, it is possible use the following mathematical relations:

$$\frac{1}{Z_L(p)}\cos(\omega t) = \mathrm{Re}\,\frac{e^{j\omega t}}{Z_L(j\omega)}$$

$$= \frac{\mathrm{Re}Z_L(j\omega)\cos(\omega t) + \mathrm{Im}Z_L(j\omega)\sin(\omega t)}{|Z_L(j\omega)|^2} \qquad (1$$

$$\frac{1}{Z_L(p)}\sin(\omega t) = \mathrm{Im}\,\frac{e^{j\omega t}}{Z_L(j\omega)}$$

$$= \frac{\mathrm{Re}Z_L(j\omega)\sin(\omega t) - \mathrm{Im}Z_L(j\omega)\cos(\omega t)}{|Z_L(j\omega)|^2} \qquad (1$$

where Re and Im stand for the real and imagina parts respectively of the associated function. Accordingly, using eqns.(16) and (17) in eqn.(1 results in:

$$i_{La} = \sqrt{2/3}\,\frac{1}{|Z_L(j\omega)|^2}$$

$$\{(v_d\ \mathrm{Re}\ Z_L(j\omega) - v_q\ \mathrm{Im}\ Z_L(j\omega))\cos(\omega t)$$

$$+ (v_d\ \mathrm{Im}\ Z_L(j\omega) + v_q\ \mathrm{Re}\ Z_L(j\omega))\sin(\omega t)\} \qquad (1$$

Substituting into eqn.(10) for i_a from eqn.(9) a i_{La} from eqn.(18) and then equating coefficients cos (ωt) and sin (ωt) yield:

$$p\, v_d = -\omega\, v_q + \frac{i_d}{C} - \frac{v_d}{C}\frac{\mathrm{Re}Z(j\omega)}{|Z(j\omega)|^2} + \frac{v_q}{C}\frac{\mathrm{Im}Z(j\omega)}{|Z(j\omega)|^2} \qquad (1$$

$$p\, v_q = \omega\, v_d + \frac{i_q}{C} - \frac{v_d}{C}\frac{\mathrm{Im}Z(j\omega)}{|Z(j\omega)|^2} - \frac{v_q}{C}\frac{\mathrm{Re}Z(j\omega)}{|Z(j\omega)|^2} \qquad (2$$

Equations (6),(7),(19) and (20) represent the f

dynamic model of the electrical part of the generator for a general load configuration.

If the load is represented by an impedance of magnitude Z_L and power factor angle ϕ, then:

$$Z_L(j\omega) = Z_L \angle \phi \qquad (21)$$

Therefore Re $Z_L(j\omega) = R_L$ and Im $Z_L(j\omega) = X_L$ such that eqns.(19) and (20) can be put in the following form:

$$p\, v_d = -\omega\, v_q + i_d/C - \{v_d \cos(\phi) - v_q \sin(\phi)\}/(C\, Z_L) \qquad (22)$$

$$p\, v_q = \omega\, v_d + i_q/C - \{v_d \sin(\phi) + v_q \cos(\phi)\}/(C\, Z_L) \qquad (23)$$

It is obvious that for a resistive load, eqns.(22) and (23) reduce to eqns(12) and (13) respectively.

At steady-state the operator p may be replaced by zero because v_d , v_q , i_d and i_q are all constants. Performing some simple mathematical treatments, steady-state relations can be obtained. It was found that these relations are in complete agreement with those attained before for both of the parametric [1,2] and the reluctance generators [8].

2-3 *Electromagnetic Torque*

The torque matrix G can be written with the aid of the transformed impedance matrix $\tilde{Z}(p)$ defined in eqn.(5). Its elements are the coefficients of the electrical angular speed ω_{re}.

Taking eqn. (4) into account , the torque matrix is given by:

$$G = \begin{bmatrix} 0 & -L_q/2 \\ L_d/2 & 0 \end{bmatrix} \qquad (24)$$

The total electromagnetic torque is given by [9]:

$$T_{em} = (P/2)\, \tilde{I}^T G \tilde{I} = (P/4) i_d\, i_q \{L_d - L_q\} \qquad (25)$$

2-4 *Mechanical Equation*

For the sake of completeness, the mechanical equation of rotational motion should be included. It takes the following form:

$$p\, \omega_{rm} = (T_{pm} - T_{em} - B_e\, \omega_{rm})/J_e \qquad (26)$$

where T_{pm} is the mechanical torque provided by the prime mover. Generally, T_{pm} depends on the mechanical angular speed ω_{rm}.

In fact, exclusion of the mechanical equation implies that the overall system inertia J_e is so high that the acceleration $p\omega_{rm}$ approaches zero. This corresponds to constant speed operation. However, in most practical cases, constant speed-operation is not possible unless a suitable control system is employed.

3- OPERATION UNDER CONSTANT GENERATOR SPEED

The differential equations describing the system dynamics have been solved. The solution is based on the fourth-order Runge-Kutta numerical method. Firstly, the program has been used to simulate the dynamic behavior under constant speed operation. The results have been checked experimentally. The laboratory setup consists of a three phase wound-rotor induction machine connected as a parametric machine. A variable capacitor bank has been used to provide self-excitation. The parametric machine was driven using a dc motor. The employed induction machine has the following nameplate data:

4 KW , 50 Hz , Y-Δ , 380/220 V, 6.9/12 A , 1410 r/min.

3-1 *Magnetic Saturation*

In the parametric machines, the magnetic saturation effect can be included in the analysis using one of the following two methods. :

1- Assuming that the axes inductances are affected by the corresponding components of the mmf. This means that L_d is a function of I_d and L_q is a function of I_q as described in [1,2].
2- Using the machine characteristics as an induction motor which can be measured by the conventional tests i.e. dc, no-load, locked rotor and open circuit tests. The details and derivation of the relationships between the two sets of

parameters (induction and parametric) are given in [5] and summarized as follows:

- $L_d = \ell_s + \ell_r + (tr + 1/tr + 2)M$
  $L_q = \ell_s + \ell_r + (tr + 1/tr - 2)M$

where:

ℓ_s and ℓ_r are the actual values of the stator and rotor leakage inductances,

M is the actual value of the magnetizing inductance, and

tr is the stator to rotor effective turns ratio.

- The relation between the magnetizing current $I_{o\mu}$ and the axes rms currents I_d and I_q is:

$$I_{o\mu} = \sqrt{(1+1/tr)^2 I_d^2 + (1-1/tr)^2 I_q^2}$$

where: $I_d = i_d/\sqrt{3}$ and $I_q = i_q/\sqrt{3}$

- The relation between the actual magnetizing inductance M and the magnetizing current can be obtained from the no-load test. Then it can be mathematically formulated using an suitable curve fitting technique.

The two methods have been applied to predict the steady state behavior of the parametric generator. Examining the published results reveals that the second method gives more satisfactory results. This superiority has been confirmed using the experimental setup under study. Therefore, the magnetic saturation effect has been included in the dynamic behavior analysis using the induction motor parameters with great confidence.

The measured parameters of the employed induction machine are:

$$R_a = 1.5\ \Omega/\text{phase}, \quad tr = 3.6,$$

$$\ell_s = \ell_{r(ref)} = 0.004\ \text{H/phase}.$$

The fitted relation between the referred value of the magnetizing inductance M_{ref} and the magnetizing current $I_{o\mu}$ is given by the following piece-wise relation:

$$M_{ref} = 0.21\ \text{H} \quad \textit{for}\ I_{o\mu} < 2.7\ \text{A}$$

$$= 0.000972\ I_{o\mu}^2 - 0.027049\ I_{o\mu} + 0.2675$$

$$\textit{for}\ 2.7\ \text{A} < I_{o\mu} < 15\ \text{A}$$

The relation is extended to over double the machine rating current (6.9 A) to ensure more accurate simulation in the normal operating conditions and to allow for the possible instantaneous high currents in the transient periods.

3-2 *Simulation and Test Results*

The following simulation and test results are obtained when the generator is driven at 1200 rpm. Self-excitation is achieved using a star-connected capacitor bank of 300 μF per phase.

Voltage Build-up

The process of self-excitation has been examined. Figure (3) shows the measured line voltage build-up at no-load compared with the results obtained using the suggested model. While Figure (4) shows the same comparison if a resistive load of 70 Ω/phase was applied before the occurrence of self-excitation. The validity of the model is evident. The ignorance of the prime mover dynamics does not greatly affect the calculated results. The experimental speed drop due to self excitation did not exceed 4%. From Figure (3) and (4), it is noted that the voltage build-up takes longer time for the loaded generator. It was noted that the self-excitation is more difficult for the loaded generator. The success of the process of self-excitation depends on the machine remanent magnetism and/or the initial charge on the capacitors terminals. These quantities represent the initial conditions required for the model to have a non-trivial solution. In practical cases, If the initial conditions are not sufficient, the self-excitation can be verified if the machine speed and/or the exciting capacitance are increased temporarily. In all cases, it is recommended to derive the generator to a suitable speed, then switch on the exciting capacitors. Once the self-excitation is achieved, the machine can be loaded.

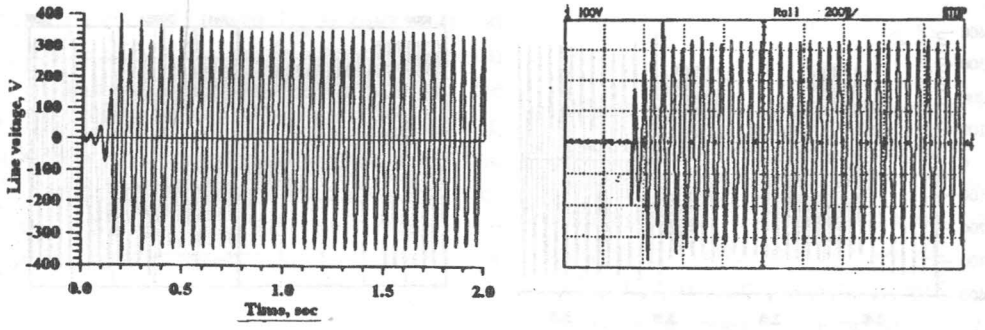

a- Theoretical *b- Experimental*

Figure 3. Voltage build-up at no-load.

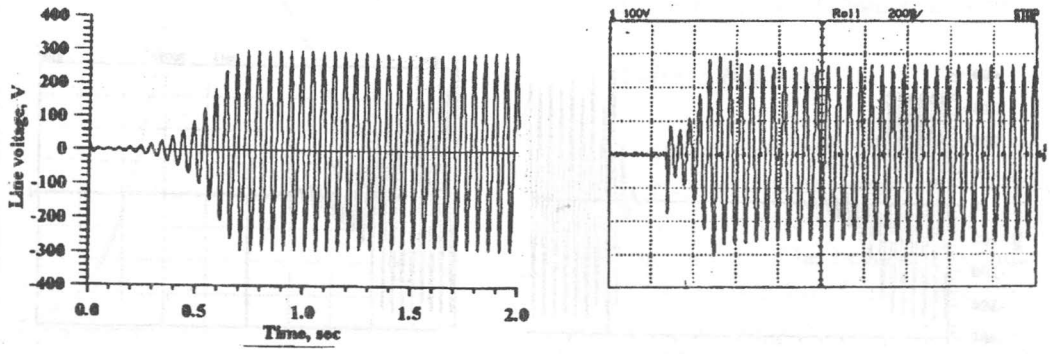

a- Theoretical *b- Experimental*

Figure 4. Voltage build-up for a resistive load of 70 Ω/phase.

Sudden Load Change

Figure (5) shows the effect of sudden application and removal of a resistive load of 70Ω/phase on the line voltage experimentally and theoretically. The validity of the suggested model is ensured. Figure (6) shows the same case for a resistive load of 40Ω/phase. The theoretical response is similar to the experimental response at the application of the load where self-excitation is lost due to this relatively heavy load. The theoretical model shows that the self-excitation can be retained if the load is removed which is not experimentally verified. Theoretically, at low magnetizing current, the mutual inductance is assumed to be constant. The electrical system in this case is linear. So, any small amount of the initial conditions can provide increasing response. During the period of heavy load application, the response decays to a small value which may be still non-zero at the instant of load removal. Therefore the self-excitation is possible. If the period of the load application is increased (e.g. doubled for the present load) in the simulation program, the response decreases to a very small value which may be numerically truncated to zero. In this case the theoretical self-excitation is not possible after load removal. Experimentally, the self-excitation needs minimum values of the initial conditions (remanent magnetism and/or initial capacitor charge) for a certain speed and exciting capacitance. Application of heavy load may cause decaying of the response to less than these minimum quantities. This requirement is owed to that the mutual inductance is not practically constant at low values of the magnetizing current. Accurate measurement of this region of the magnetizing curve is practically difficult.

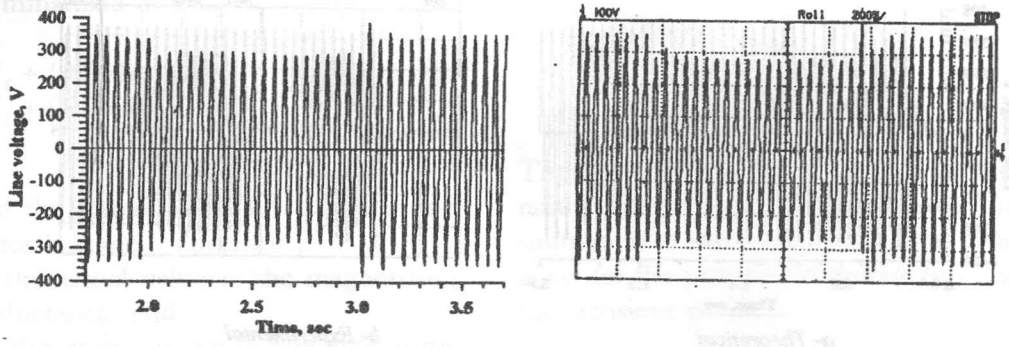

a- Theoretical *b- Experimental*

Figure 5. Sudden application and removal of a resistive load of 70 Ω/phase.

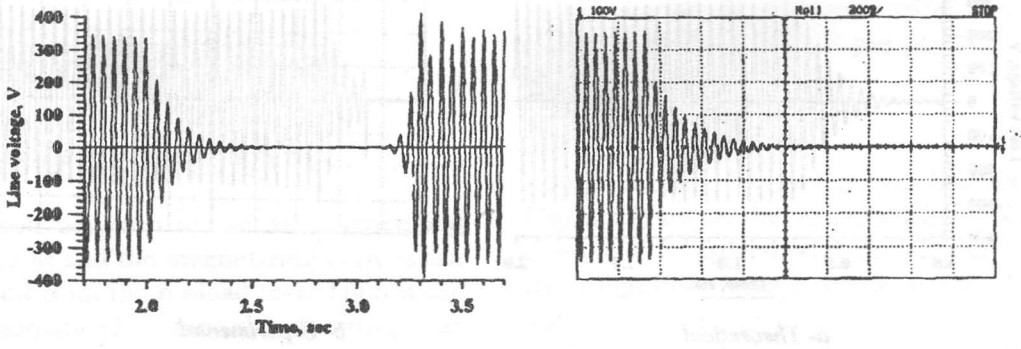

a- Theoretical *b- Experimental*

Figure 6. Sudden application and removal of a resistive load of 40 Ω/phase.

4- APPLICATION IN A WIND ENERGY SYSTEM

Based on the validity of the suggested mathematical model, the performance of the parametric generator has been investigated when it is connected to a wind turbine to supply an isolated load. The computer program was modified to simulate the operation under both of constant wind speed and wind gusting conditions.

4-1 *Wind Turbine Characteristics*

For a certain turbine, the amount of wind power converted into mechanical power P_w depends on the wind speed V_w, air density ρ, blades' diameter D and the power coefficient C_p according to the following relation [10]:

$$P_w = 1/8\ \pi\ \rho\ D^2\ V_w^3\ C_p$$

The power coefficient C_p of the wind turb depends on its design (*e.g. blades' diameter, sh and pitch angle)* along with the tip-speed ratio λ is defined as the ratio between the speed at blade tip and upstream wind speed V_w. T tip-speed ratio is expressed mathematically follows:

$$\lambda = \frac{\pi D N_t}{60 V_w}$$

where N_t is the speed of the wind turbine shaf rpm.

The employed wind turbine [10] has a bl diameter of 2.75 m. Figure (7) shows dependence of the power coefficient on

tip-speed ratio of this typical wind turbine. It is obvious that the extracted power P_w is maximum at one optimum value of λ. If variable speed operation is possible, a suitable control system can be employed to adjust λ at its optimum value according to the variation of the wind speed. However if the rotor speed is to be held constant, extracting power from wind can be maximized by using the mechanical pitch angle control.

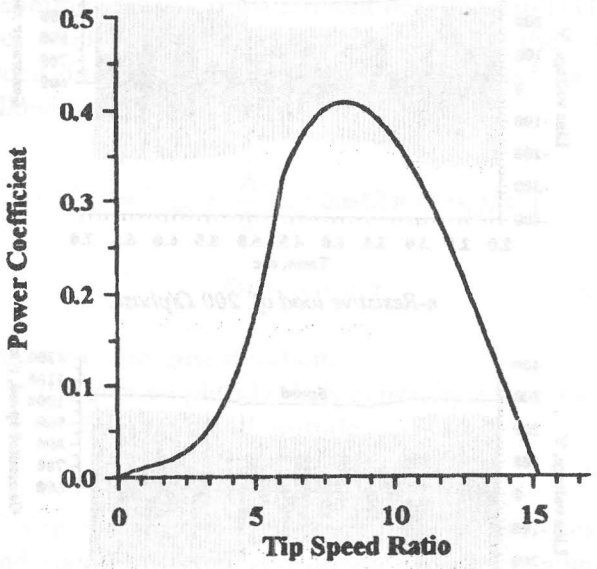

Figure 7. C_p-λ characteristics of a typical wind turbine [10].

For a certain wind speed V_w , the speed N_o of the unexcited generator is to be evaluated. This speed is considered the initial rotor speed of the simulation run. Assume that the mechanical system is in steady state (constant rotating speed) before the period under investigation ($t < 0$). Hence N_o can be computed with the aid of the mechanical equation of motion and the turbine characteristics C_p-λ. This results in a nonlinear algebraic equation that can be solved to obtain N_o for certain system parameters. The problem can be greatly simplified to obtain an acceptable approximate solution by considering the damping coefficient B = 0. Therefore the required deriving torque tends to zero. Hence C_p = zero. Therefore the turbine operates at its maximum tip speed ratio λ (λ_{max}). Using eqn.(28), the required speed N_o can be calculated from the following simple relation:

$$N_o = \frac{60 n \lambda_{max}}{\pi D} V_w \qquad (29)$$

where n is the ratio between generator and turbine speeds i.e. pulley or gear ratio. In order to obtain suitable generator speeds, a pulley ratio of 2 is considered. This value achieves initial generator speed of 1200 rpm for wind speed of 6 m/s. This enables fair comparison between the case of constant generator speed operation (excluding mechanical equation) and the case of constant wind speed operation.

4-2 *Constant wind speed condition*

Voltage Build-up

The process of self-excitation has been examined for operation under constant wind speed of 6 m/s and initial generator speed of 1200 rpm (before self-excitation.) The behavior is shown in Figure (8). The line voltage build-up of the unloaded generator is shown in Figure (8a). The effect of the prime mover dynamics is evident if the response is compared with the case of constant generator speed of 1200 rpm shown in Figure (3). For the wind-driven generator, the steady state no-load voltage drops by 31.4% due to speed drop of 14.2% (from 1200 to 1030 rpm).

Figure (8b) shows the voltage build-up if the generator was loaded before self-excitation with a resistive load of 200 Ω/phase, while Figure (8c) shows the same case if the load is inductive of 200 Ω/phase impedance and 0.8 power factor. Higher values of voltage and speed drops are obtained for the loaded generator compared with the no-load case. Figure (8b) shows a speed drop of 19.2% which causes a voltage drop of 48.8% compared with the case of constant speed prime mover speed at 1200 rpm (not shown). The corresponding values of drop in Figure (8c) are 16.75% for speed and 49.2 for voltage.

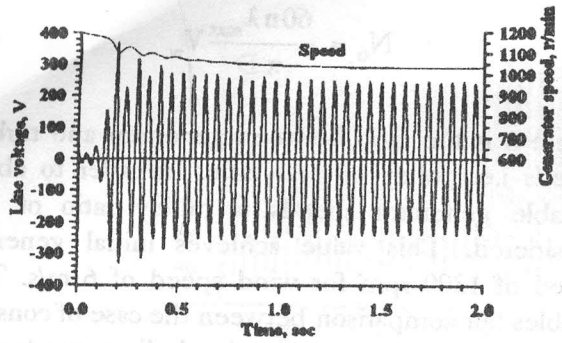

a- *No-load*

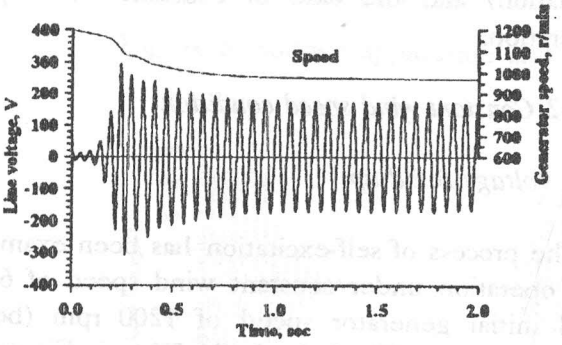

b- Resistive load of 200 Ω/phase.

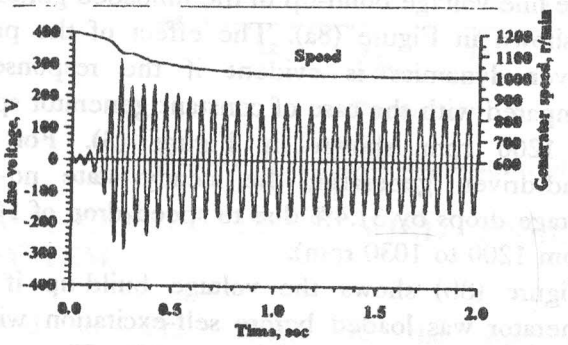

c- Inductive load of 200 Ω/phase impedance and 0.8 power factor.

Figure 8. Voltage build-up at constant wind speed of 6 m/s.

Sudden Load Change

Figure (9) shows the behavior of the wind-driven generator under the application and removal of load. Figure (9a) shows the response if the load is resistive of 200 Ω/phase, while Figure (9b) shows the response if the load is inductive of 200 Ω/phase and 0.8 power factor. The expected drops in speed and terminal voltage are obvious.

Figure (9c) shows the line voltage response the application of a relatively heavy load res load of 40Ω/phase which results in a failure i self-excitation which causes a speed increase 1030 to 1080 rpm. Removal of this heavy loac cause retaining self-excitation if the capacitor c and/or remanent magnetism have suitable valu discussed in Section 3.2.

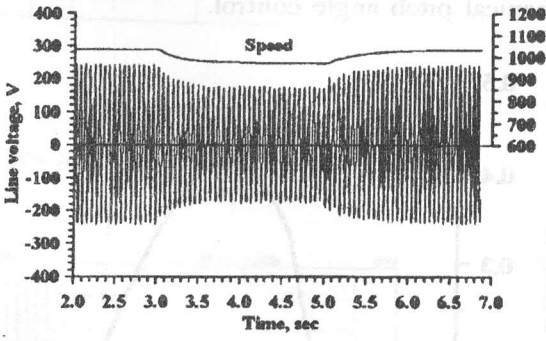

a-*Resistive load of 200 Ω/phase.*

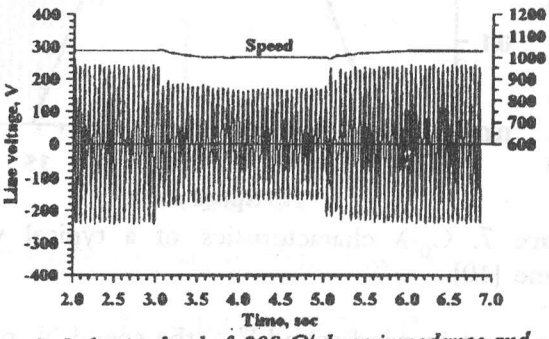

b- Inductive load of 200 Ω/phase impedance and 0.8 power factor.

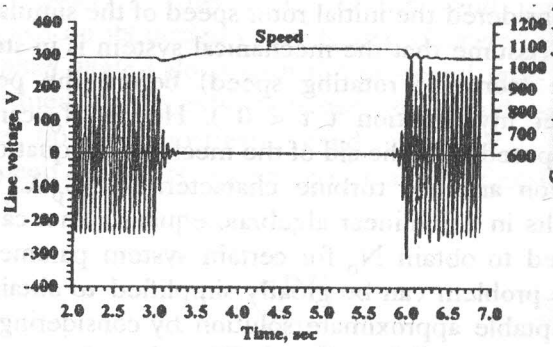

c- Resistive load of 40 Ω/phase

Figure 9. Sudden application and removal of l of 70 Ω/phase at constant wind speed of 6 m/

4-3 *Wind gusting condition*

Assumption of constant wind speed is acceptable only if the time under consideration is relatively small. Wind speed is continuously varying in a stochastic manner. This causes difficulties in mathematical formulation. Therefore time variation of wind speed can be assumed to be of a series of discrete gusts of different amplitudes and duration. Each gust has been mathematically expressed using recommendations provided and described in [11]. If the wind speed before gusting is V_{wo}, then the speed during the gust V_{wg} can be expressed by the following relation :

$$V_{wg} = V_{wo} + \frac{A}{2}\{1+\cos(2\pi\,(t-t_o)/\tau)\}$$

$$for\ t_o < t < \tau \qquad (30)$$

where τ is the gust duration.

A is the gust amplitude. It is generally a function of gust duration τ and altitude.

t_o is the time at which the gust starts.

Consider a wind gust of amplitude A= 30 % over a wind speed of 6 m/s, and duration τ= 2 sec. Figure (10a) shows terminal line voltage and winding phase current response for unloaded generator if the gust begins at t=3 sec. Figure (10b) shows the same response when the generator is loaded by a resistive load of 200 Ω/phase. Figure (10c) shows the response for inductive load of 200 Ω/phase impedance and 0.8 power factor.

It is noted that such a gust results in an increase of 65% in the terminal voltage of the unloaded generator. This percentage increases for loaded generator to be 79.9 % in Figure (10b) and 90.7% in Figure (10c). This is because of the increase in the generator speed that is 22.6% in Figure (10a) and about 18.7% for both of Figure (10b) and Figure (10c). Also It is noted that winding current is more affected by the wind gust. An increase of 94 % occurs for the unloaded generator and 111.7% for the case of resistive load shown in Figure (10b). The percentage reaches 124% in the case of the inductive load shown in Figure (10c). This shows that wind gusts may result in dangerous effects. However these effects can be reduced by increasing the total system inertia. It was found that if system inertia is doubled, the speed increases by 18.4% instead of 22.6%. and the increase in the terminal voltage becomes 50% instead of 65%. Also increase in the winding current becomes 75.5% instead of 94%. This is because of the increase in the system stored kinetic energy that helps in absorbing the mechanical system disturbances.

Generally the dynamic behavior of the self -excited parametric generator is similar to that of self-excited induction generator. So its controlled behavior can be achieved in a similar way. As a wind driven generator, the speed can be kept constant by using a suitable mechanical pitch angle control. This enables connection of the generator to the grid as in the case of the wind driven synchronous generators [11].

6- CONCLUSIONS

A dynamic model of the self-excited stand-alone wound-rotor parametric generator has been developed. The derivation of the machine dynamic equations is based on transforming the actual equations to the synchronously rotating reference frame. Then a full system model is derived using the actual relations between machine, exciting capacitance and load equations. The results have been checked experimentally resulting in a satisfactory agreement.

As an application of the suggested model, the dynamic behavior is investigated when the generator is connected to a wind turbine. The results show the importance of considering the prime mover characteristics. Also the results show the dangerous effect of wind gusting conditions. It was found that a gust of 30 % amplitude may cause an increase in the terminal voltage by 65% at no-load. This percentage increases with loading to over 90%. The corresponding increase in the winding current is from 94% at no-load to over 120% with loading. This effect can be reduced by increasing the system inertia on the account of response speed.

The controlled behavior of the stand-alone self-excited parametric generator can be achieved in a similar way to that of the stand-alone self-excited induction generator.

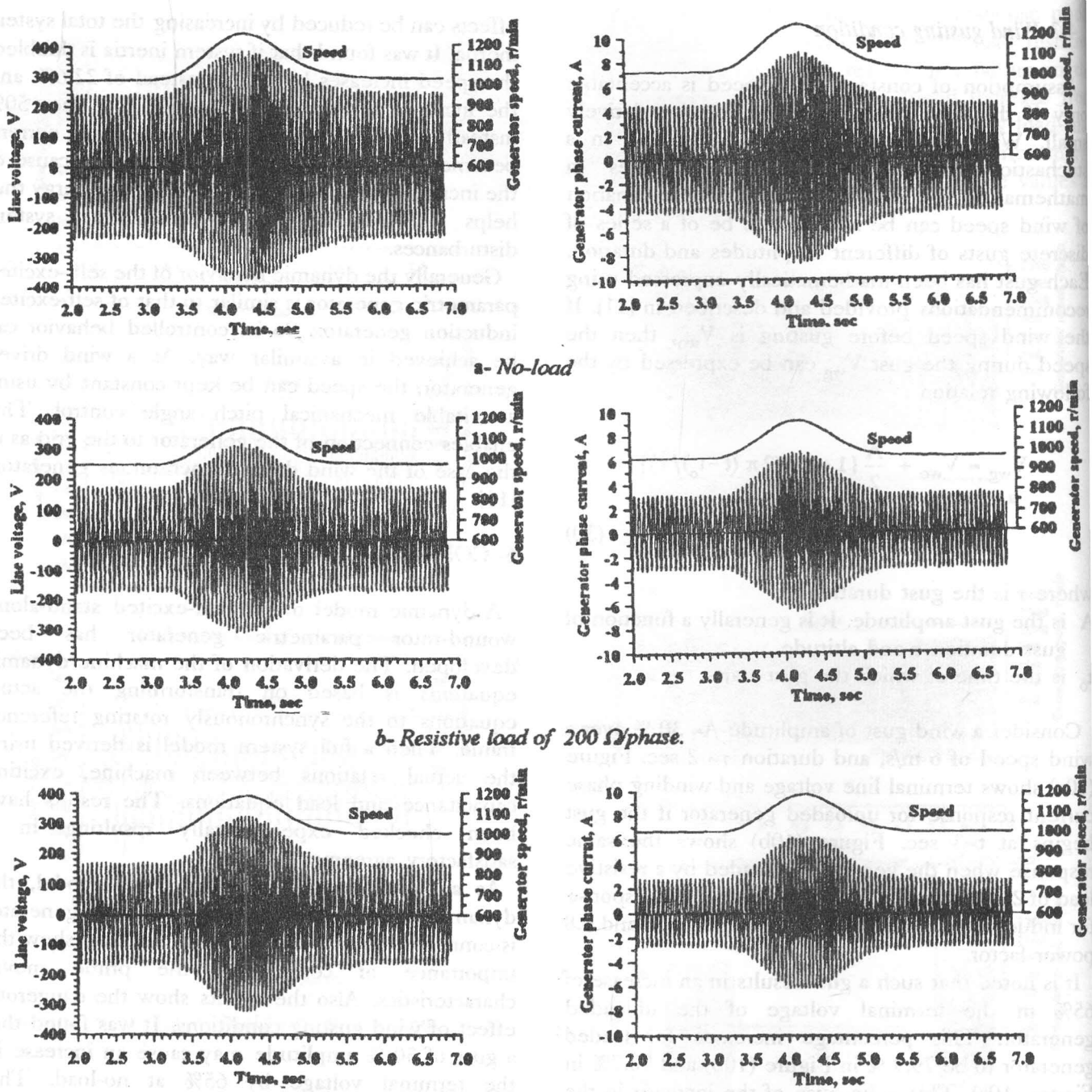

a- *No-load*

b- *Resistive load of 200 Ω/phase.*

c- *Inductive load of 200 Ω/phase impedance and 0.8 power factor.*

Figure 10. Operation at wind gusting condition of 30% amplitude and 2 s duration.

In wind energy conversion applications, the parametric generator can be treated as a synchronous generator. This suggests the use of pitch angle mechanical control of the driving wind turbine. This can keep the generator speed constant to provide electrical power of constant frequency. In this case, connection with the common grid is possible.

The suggested model of the parametric generator will be greatly useful in selecting and designing the suitable control method to achieve more satisfactory performance.

REFERENCES

[1] A.S. Mostafa, A.L. Mohamadein and E.M. Rashad, "*Application of Floquet's theory to the analysis of series-connected wound-rotor self-excited synchronous generator*", IEEE Trans. on EC, vol. 8 No. 3, Sept. pp 369-376, 1993.

[2] A.S. Mostafa, A.L. Mohamadein and E.M. Rashad, "*Analysis of series-connected wound-rotor self-excited induction generator*", IEE Proc. B , Vol. 140, No. 5, Sept. 1993, pp 329-336.

[3] A.L. Mohamadein and E.A. Shehata, "*Theory and performance of series-connected wound-rotor self-excited synchronous generators*", IEEE Trans. on EC, Vol. 10, No. 3 Sept. 1995, pp 508-515.

[4] E.A. Shehata, "*Comparison between controlled performance of self-excited induction and series-connected synchronous generators*", M.Sc. Thesis, Alexandria University, Oct. 1992.

[5] Y.G. Desouky, "*Voltage control of self-excited series-connected synchronous generator*", M.Sc. Thesis, Alexandria University, Oct. 1993.

[6] M.M. El-Shanawany, "*Capacitor controlled self-excited series-connected synchronous generator.*", Engg. Research Bulletin, Faculty of Engg., Menoufyia University, Egypt, Vol. 17, Part I, 1994, pp 209-225.

[7] E.M. Rashad, M.E. Abdel-Karim and Y.G. Desouky, "*Theory and analysis of three phase series-connected parametric motors*", IEEE-PES Summer Meeting , July 28- August 1 1996, in Denver, Colorado, USA

[8] A.L. Mohamadein, Y.H.A. Rahim and A.L. Al-Khalaf, "*Steady-state performance of self-excited reluctance generators*", IEE Proc. B, Vol. 137, No. 5, Sept. 1990, pp 293-298.

[9] N.N. Hancock, "*Matrix analysis of electric machinery*" , (book) Pergamon, 2nd Edition , 1974

[10] C.S. Brune, R. Spee and A.K. Wallace, "*Experimental evaluation of a variable-speed, doubly-fed wind-power generation system*", IEEE Trans. on IA, Vol. 30 No. 3, May/June 1994, pp 648-655.

[11] H. Hwang and L.J. Gilbert, "*Synchronization of wind turbine generators against an infinite bus under gusting wind conditions*", IEEE Trans. on PAS, Vol. 97, No.2, March/April 1978, pp 536-544.